sion paths were maintained by connecting the corresponding input and output ports with 1 × 4 fibre couplers. Ports a and b were assigned as four available input and four available output ports, respectively.
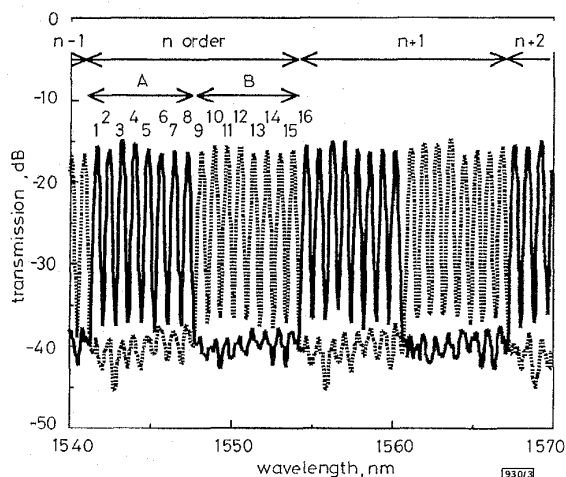

Fig. 3 *Spectral response of two dropped wavelength groups A and B*

A: when combination of switches 1, 2, 3, 4 and 6 is selected
B: when combination of switches 1, 2, 3, 4 and 5 is selected

Fig. 3 shows the measured spectral response of the fabricated WCGDF. The spectra are characterised by two wavelength groups of eight transmission peaks with a 0.8 nm (100 GHz) wavelength spacing. Wavelength group A {λ1, ..., λ8} was dropped by selecting the combination of switches 1, 2, 3, 4 and 6. Another wavelength group B (λ9, ..., λ16) was dropped by selecting another combination of switches 1, 2, 3, 4 and 5. Fig. 4 shows the spectral response of four different groups. Wavelength group C {λ1, λ2, λ3, λ4} was dropped when the transmission path was selected by turning on switches 1 and 6. Next, wavelength group D {λ5, λ6, λ7, λ8} was dropped by switching on switches 3, 4, and 6. Finally, wavelength groups E {λ9, λ10, λ11, λ12} and F {λ13, λ14, λ15, λ16} were dropped by turning on the corresponding switches as shown in Fig. 2. An interesting feature is that these spectral responses exhibit other grating orders. If required, it is possible to use a periodic spectral response. Slight loss deviation occurred because the splitting ratios in the couplers were not identical. As a result the proposed WCGDF operated in accordance with the design. The fibre-to-fibre insertion loss in the fabricated WCGDF was 15 – 17 dB. Interchannel crosstalk was < –20 dB. These values are acceptable for constructing dense WDM networks using optical fibre amplifiers.
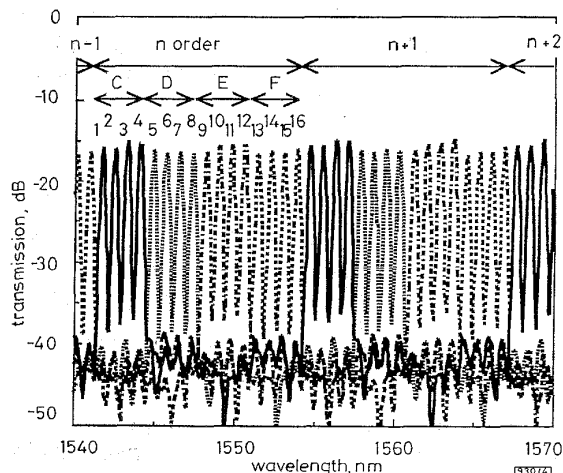

Fig. 4 *Spectral response of four dropped wavelength groups*

C: when selected by turning on switches 1, 2 and 6
D: when selected by turning on switches 3, 4 and 6
E: when selected by turning on switches 1, 2 and 5
F: when selected by turning on switches 3, 4 and 5

Conclusion: A novel WDM-channel group drop filter was proposed and successfully demonstrated by using a single silica-based arrayed-waveguide grating 16 × 16 multiplexer, couplers and switches. This smart tunable WDM-channel group drop filter is expected to be used for constructing dense WDM networks and other such applications.

Y. Tachikawa and Y. Inoue (*NTT Opto-electronics Laboratories, Shirokata 162, Tokai-Mura, Naka-Gun, Ibaraki-ken 319-11, Japan*)

References

1 SMIT, M.K.: 'New focusing and dispersive planar component based on an optical phased array', *Electron. Lett.*, 1988, **24**, pp. 385–386
2 TAKAHASHI, H., SUZUKI, S., and NISHI, I.: 'Multi/demultiplexer for nanometer-spacing WDM using arrayed-waveguide grating'. Dig. Conf. Integrated Photonics Research, OSA, Washington DC, 1991, Paper PD-1
3 DRAGONE, C.: 'An N×N optical multiplexer using a planar arrangement of two couplers', *IEEE Photonics Technol. Lett.*, 1991, **3**, pp. 812–815
4 TACHIKAWA, Y., INOUE, Y., KAWACHI, M., TAKAHASHI, H., and INOUE, K.: 'Arrayed-waveguide grating add-drop multiplexer with loop-back optical paths', *Electron. Lett.*, 1993, **29**, (24), pp. 2133–2134
5 ZIRNGIBL, M., and JOYNER, C.H.: 'High performance, 12 frequency optical multichannel controller', *Electron. Lett.*, 1994, **30**, (9), pp. 700–701
6 ISHIDA, O.: 'FDM-channel selection filter using arrayed-waveguide grating multiplexer', *Electron. Lett.*, 1995, **30**, (25), pp. 2154–2155
7 BRACKETT, C.A., ACAMPORA, A.S., SWEITZER, J., TANGONAN, G., SMITH, M.T., LENNON, W., WANG, K.-C., and HOBBS, R.H.: 'A scalable multiwavelength multihop optical network: A proposal for research on all-optical networks', *J. Lightwave Technol.*, 1993, **LT-11**, (5/6), pp. 736–753
8 INOUE, Y., OHMORI, Y., KAWACHI, M., ANDO, S., and SAWADA, T.: 'Polarization-insensitive arrayed-waveguide grating multiplexer with polyimide waveplate as TE/TM mode converter'. Dig. Conf. Integrated Photonics Research (IPR'94), San Francisco, 1994, Paper ThF14
9 KAWACHI, M.: 'Silica waveguides on silicon and their application to integrated-optic components', *Opt. Quantum Electron.*, 1990, **22**, pp. 391–416

Ultrahigh-bandwidth (42 GHz) polarisation-independent ridge waveguide electroabsorption modulator based on tensile strained InGaAsP MQW

K. Satzke, D. Baums, U. Cebulla, H. Haisch, D. Kaiser, E. Lach, E. Kühn, J. Weber, R. Weinmann, P. Wiedemann and E. Zielinski

Indexing terms: Harmonic generation, Optical fibres

Electroabsorption modulators with polarisation independence of chirp and transmission (TE/TM sensitivity <0.4 dB at 1550 nm) over a wide wavelength range from 1540 nm to 1560 nm have been realised using tensile strained InGaAsP quantum wells. The fabricated devices show 42 GHz modulation bandwidth and 1.8 V drive voltage, resulting in a high bandwidth-to-drive-voltage ratio of 23.3 GHz/V.

Introduction: There is increasing interest in external modulators with ultra-high bandwidth and low drive voltage for optical telecommunications systems operating in the 1.55 µm region. Among these, the multiple quantum well (MQW) electroabsorption (EA) modulator is one of the most promising candidates.

Applications for MQW EA modulators range from multigigabit TDM and OTDM, long-haul terrestrial and submarine fibre transmission systems to optical demultiplexing stages. Demultiplexing applications, especially, require the modulator transmission to be insensitive to polarisation because optical polarisation control is very difficult to achieve in fibre transmission lines. An extrapolated small-signal bandwidth of up to 50GHz with InGaAs/InAlAs MQW EAM [1] and 20Gbit/s transmission over 100km dispersion shifted fibre [2] have been demonstrated. MQW EA modulators have also been applied for efficient soliton generation and coding [3].

Polarisation-independent modulation can be achieved with the introduction of tensile strain into the wells, taking advantage of the degeneracy of a heavy-hole and light-hole exciton peak of the MQW material [4]. Polarisation sensitivity of <1dB was demonstrated for the first 3dB of extinction [5].

Device structure: The quantum wells were designed for polarisation independence at a target wavelength of 1550nm. This was achieved by careful adjustment of well width and amount of tensile strain such that heavy- and light-hole transition wavelengths match at 1.51µm. The *pin* structure was grown by LP-MOVPE on an n^+-InP substrate. The undoped MQW layer stack consists of eight periods of 0.38% tensile strained InGaAsP wells with unstrained InGaAsP barriers. The layer stack is topped by a 2.5µm-thick *p*-InP and a p^+-InGaAs contact layer.

First, deep ridge waveguides of 3µm widths were realised by a combination of dry and wet etching. Polyimide was spin-coated to minimise the stray capacitance of the bond pad. Devices with a total length of 120µm were cleaved, soldered on a 50Ω matched AIN submount, bonded and characterised.
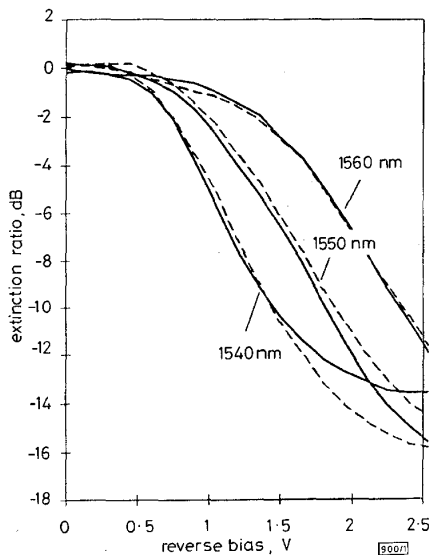

Fig. 1 *Extinction ratio characteristics against externally applied reverse bias measured at 1540, 1550 and 1560nm*

——— TE
– – – – TM

Static characteristics: Extinction characteristics at 1540, 1550 and 1560nm wavelengths are shown in Fig. 1. At 1550nm, only 1.8V drive voltage is needed for 10dB extinction. The maximum extinction ratio with 2.5V at 1550nm was 16dB. The dependence of polarisation sensitivity observed in the extinction ratio is small even at high extinction ratios >10dB. More important is the polarisation independence of the fibre-to-fibre insertion loss in the on-state. Figure Fig. 2 gives the difference between TE and TM polarisation for insertion loss and extinction ratio. At the target wavelength of 1550nm the polarisation sensitivity is <0.4dB for extinction ratios up to 10dB. The polarisation sensitivity stays below 1dB in the total wavelength range of 1540 to 1560nm.

Dynamic characteristics: The small-signal frequency response shown in Fig. 3 was recorded using a 50GHz network analyser and a calibrated photodiode. The measured electrical −3dB band-

width of the 120µm-long device is 42GHz. Measurements performed in the TE and TM modes showed no influence of the input polarisation state on bandwidth. The bandwidth-to-drive-voltage
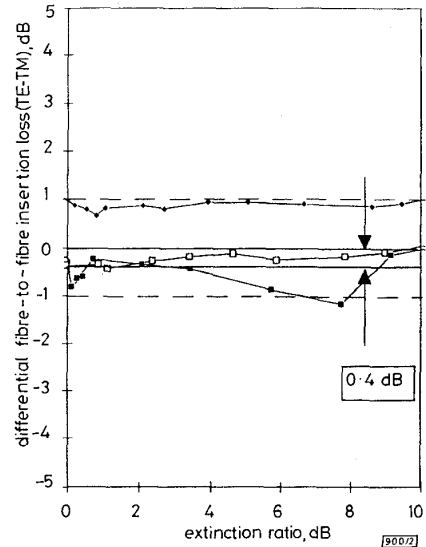
Fig. 2 *Difference in fibre-to-fibre insertion loss between TE and TM polarisation against extinction ratio, measured at 1540, 1550 and 1560nm*

● 1560nm: TE-TM < 1dB
□ 1550nm: TE-TM < 0.4dB
■ 1540nm: TE-TM < 1dB

ratio is 23.3GHz/V at 1550nm, which exceeds the best values reported so far for MQW EA modulators with quaternary wells [6].

The small frequency response curve was fitted using an RLG model, yielding a device resistance of $R = 13\Omega$, a device capacitance of $C = 145\text{fF}$ and a bond wire inductance of $L = 0.17\text{nH}$. These parameters are consistent with data obtained in static measurements. This leads to the conclusion that the modulation speed of the device is limited by its capacitance.

Table 1: Reverse bias voltage required for 10dB extinction ratio and for negative chirp parameter α_H

Operation wavelength, nm	1540	1550	1560
Bias for neg. α_H parameter, V	1.5	2.0	2.5
Bias for 10dB extinction, V	1.3	1.8	2.3
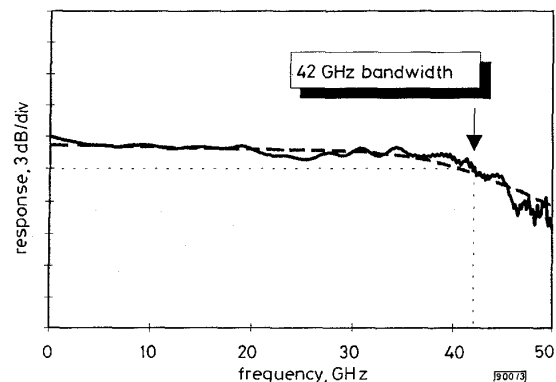
Fig. 3 *Frequency response of 120µm-long uncoated device under 1.8V reverse bias and* $\lambda = 1557nm$

– – – – calculated, with device capacitance of 145fF
——— measured

Chirp parameter: The chirp parameter $\alpha_H = 2d\phi/d\ln I$ (where ϕ is the output light phase and I its intensity) was measured using the

fibre response peak method [7]. Reverse bias voltages required for 10dB extinction ratio and for negative α_H are summarised in Table 1. From the measured chirp parameter and extinction ratio, phase-intensity diagrams for TE and TM polarisation have been calculated by numerical integration of the above equation (see Fig. 3). At 1550nm, the phase change is slightly lower for TM polarisation. At 1560nm the phase of output light for TE and TM polarisation are practically identical, which should result in standard fibre transmission performance independent of the modulator input polarisation.
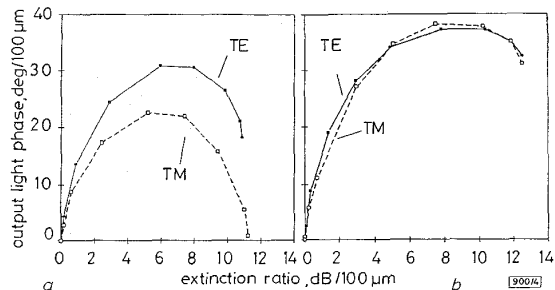

Fig. 4 *Output light phase against extinction ratio of 120μm-long modulator device for TE and TM mode at 1550 and 1560nm*

a 1550nm
b 1560nm

Conclusions: An ultra-high modulation bandwidth of 42GHz and low driving voltage of 1.8V was achieved in an EA modulator incorporating tensile strained InGaAsP MQW, taking advantage of the reduced capacitance of the deep-ridge lateral structure. Low polarisation sensitivity (0.4dB at 1550nm, <1dB from 1540 to 1560nm) of insertion loss, extinction ratio and output phase have been demonstrated. Thus this device shows great potential as transmitter and demultiplexer for next generation 40Gbit/s (O)TDM and 4 × 40Gbit/s OTDM transmission systems.

18 September 1995

K. Satzke, D. Baums, U. Cebulla, H. Haisch, D. Kaiser, E. Lach, E. Kühn, J. Weber, R. Weinmann, P. Wiedemann and E. Zielinski (*Alcatel Corporate Research Centre Stuttgart, Optoelectronic Components Division, Dept. ZFZ/WO, Lorenzstr. 10, D-70435 Stuttgart, Germany*)

References

1 IDO, T., TANAKA, S., SUZUKI, M., and INOUE, H.: 'An ultra-high-speed (50GHz) MQW electro-absorption modulator with waveguides for 40Gbit/s optical modulation'. Proc. IOOC'95, Paper PD1-1, pp. 1–2

2 KATAKOA, T., MIYAMOTO, Y., WAKITA, K., and KOTAKA, I.: 'Ultrahigh-speed driverless MQW intensity modulator, and 20Gbit/s 100km transmission experiments', *Electron. Lett.*, 1992, **28**, pp. 897–898

3 SOULI, N., DEVAUX, F., RAMDANE, A., KRAUZ, P., OUGAZZADEN, A., HUET, F., CARRÉ, M., SOREL, Y., KERDILES, J.F., HENRY, M., AUBIN, G., JEANNY, E., MONTALLANT, T., MOULU, J., NORTIER, B., and THOMINE, J.B.: '20Gbit/s high performance MQW TANDEM modulators for soliton generation and coding', *IEEE Photonics Technol. Lett.*, 1995, **7**, (6), pp. 629–631

4 RAVIKUMAR, K.G., AIZAWA, T., SUZAKI, S., and YAMAUCHI, R.: 'Observation of polarization independent electric-field effect in InGaAs/InP tensile-strained quantum well and its proposal for optical switch', *Appl. Phys. Lett.*, 1992, **61**, (16), pp. 1904–1906

5 DEVAUX, F., CHELLES, S., OUGAZZADEN, A., MIRCEA, A., CARRÉ, M., HUET, F., CARENCO, A., SOREL, Y., KERDILES, J.F., and HENRY, M.: 'Full polarisation insensitivity of a 20Gb/s strained-MQW electroabsorption modulator', *IEEE Photonics Technol. Lett.*, 1994, **6**, (10), pp. 1203–1206

6 DEVAUX, F., DORGEUILLE, F., OUGAZZADEN, A., HUET, F., CARRÉ, M., CARENCO, A., HENRY, M., SOREL, Y., KERDILES, J.F., and JEANNY, E.: '20Gbit/s operation of a high-efficiency InGaAsP/InGaAsP MQW electroabsorption modulator with 1.2V drive voltage', *IEEE Photonics Technol. Lett.*, 1993, **5**, (11), pp. 1288–1290

7 DEVAUX, F., SOREL, Y., and KERDILES, J.F.: 'Simple measurement of fibre dispersion and of chirp parameter of intensity modulated light emitter', *J. Lightwave Technol.*, 1993, **LT-11**, (12), pp. 1937–1940

Effective stimulated Brillouin gain in singlemode optical fibres

J. Botineau, E. Picholle and D. Bahloul

Indexing terms: Stimulated Brillouin scattering, Nonlinear optics, Optical fibres

Transverse material inhomogeneities yielding the guiding properties of any optical fibre also cause a variation of stimulated Brillouin resonance frequency, and thus a spectral broadening as well as a reduction of the overall SBS gain. A simple model defines an effective steady SBS gain, and may explain the dispersion of available measured values.

Stimulated Brillouin scattering (SBS) is the resonant interaction between an incident laser 'pump' wave, a backscattered 'Brillouin' lightwave, and an induced hypersonic 'acoustic' wave [1, 2]. It presents many interesting features, such as the very high coherence of SBS fibre lasers, but is mainly considered a hindrance to optical transmissions. The SBS gain g_B in a given fibre is a key parameter, which should be evaluated with good precision. Nevertheless, available measurements still prove a very large dispersion from the admitted values, commonly tens of percent [3, 4], but sometimes within more than one order of magnitude [5], and are always lower than the value obtained in the bulk. Such discrepancies arise from two major failures of the usual unidimensional model of SBS in singlemode fibres: (a) the acoustic damping rate γ_a is usually deduced from values obtained in bulk silica; this neglects both the coupling losses between longitudinal and torsional acoustic waves, which may be induced in fibre by cabling or other mechanical constraints, and the diffraction losses, which may be important in acoustically antiguiding fibres; (b) the gain reduction relative to the transverse material gradient in any optical fibre. In this Letter, we consider only the latter, usually neglected, and show that in the stationary regime it may be described through an effective SBS gain g_B^{eff}, which strongly depends on the fibre transverse doping distribution and may lead to a notable reduction of its bulk value; this reduction is not due to local variations of the SBS coupling efficiency, but to a shift of the resonance conditions.

The fibre inhomogeneities can be addressed from two complementary points of view. The material damping time may be long enough for the wave to spread on the acoustic modes of the fibre, which behaves as a multimode acoustic waveguide, even for optically singlemode fibres [6]. Then, if the SBS interaction is slow compared to this spreading, the transverse structure can be taken into account through a simple overlap integral between optical and acoustic modes [7]. The acoustic velocity is, however, usually too low for the acoustic modes to set up within nanoseconds, and such correction may become relevant only at long wavelengths, where γ_a is much smaller. We use here the opposite approximation, and neglect the propagation of the acoustic wave, so that its intensity depends only on the local optical intensities, but still in the frame of a coherent 3-wave model of SBS, which can only describe the interaction out of the exact resonance [2]. Let us consider a cylindrical singlemode optical fibre, ρ being the radial distance to the axis; the doping concentration gradient yields ρ-dependent material properties, namely the local acoustic velocity c_a^ρ and the optical index n^ρ. The electromagnetic field distribution F^ρ (with an arbitrary normalisation) and the effective index n_{eff} are both considered identical for the two optical components. Two monochromatic contrapropagating (pump and Brillouin) waves propagate along the fibre, with the frequencies $\omega_{p,B}$ and the propagation constants $k_{p,B} = (n_{eff}/c)\omega_{p,B}$, i.e. in a stationary regime,